Pergamon

Cement and Concrete Research, Vol. 27, No. 8, pp. 1225-1235, 1997
© 1997 Elsevier Science Ltd
Printed in the USA. All rights reserved
0008-8846/97 $17.00 + .00

PII S0008-8846(97)00111-7

# RELATIONSHIP BETWEEN PORE STRUCTURE AND PERMEABILITY OF HARDENED CEMENT MORTARS: ON THE CHOICE OF EFFECTIVE PORE STRUCTURE PARAMETER

**L'. Bágel' and V. Živica**
Institute of Construction and Architecture of the Slovak Academy of Sciences, Dúbravská cesta 9, 842 20 Bratislava, Slovak Republic

(Refereed)
(Received October 4, 1995; in final form June 6, 1997)

## ABSTRACT

An experimental study has been performed with the aim of quantifying pore structures systems of cement mortars and correlating them with water permeability. A new pore structure parameter has been found to predict the permeabilities of mortars with an acceptable accuracy. A reasonably close correlation was found between the structural parameter and the permeability if the "relevant" pore size range was incorporated into the functional equation which expresses the relation between the pore structure and permeability. *© 1997 Elsevier Science Ltd*

## Introduction

Many important properties, such as strength, corrosion resistance, durability and permeability are closely related to the pore structures of cement-based materials. For the determination of usable relationship between pore structure and permeability it is necessary to choose the suitable pore structure parameters. It is generally accepted that the total porosity, as the basic structural parameter, appears not to be a significant measure for an evaluation of water permeability (1,2), because the water flow is influenced mainly by the pore size distribution rather than by the total pore volume.

The permeability of a cement composite is now accepted mainly to be a function of pore size distribution (3-5) and a wide variety of pore size parameters (average size of pores) were presented in literature to more precise characterizing the distribution of pores: "hydraulic radius" (1,6), "threshold diameter" (4,7), "maximum continuous pore radius" (3). One of the most useful parameters has proved to be the "critical pore radius" (8), but in most cement-based materials this parameter and the "pore radius median" have similar values. Meng (9) defined new term "relevant porosity" characterizing the voids available for water transport. The relevant porosity fraction comprising the pore volume with radii over 100nm is in fact the same as the down level of the capillary porosity having a major effect on water flow which was presented previously (4,5). Mercury intrusion porosimetry is a common method used to determine pore size distribution.

A number of models and theories have been suggested in detail in previous studies to predict permeability coefficient of porous material from structural data (6,10-13). Brown et al. (14) presented a significant critical review and description of different pore structure and permeability measurement methods and models including their advantages and limitations with regard to their application to cementitious materials.

There are three known equations based on empirical models, which were presented recently to obtain the usable relation between permeability and pore structure (1,3,4). However, not all different structural parameters used in these relationships were estimated by mercury intrusion porosimetry (MIP). To the authors opinion there has been a possibility the predicting of permeability coefficient on the base of more simple combined pore structure parameter at which all individual members of this parameter are from only MIP data obtained.

In spite of a great deal of research, the practical application of the existing empirical formulas to predicting of concrete permeability remains very insufficient. The present paper—in the light of existing knowledge and recently presented conclusions—describes theoretical conclusions which are based on experimental results and has the main reason—to define and interpret the simple pore structure parameter and to estimate the range of pores which are predominantly related to permeability i.e., the "relevant" pore size range.

## Experimental

Preparation of Specimens. Cylindrical specimens of nine mortar mixes with different water/cement and sand/cement ratios, 150mm in diameter and 30mm thick were prepared from ordinary Portland cement (CEM I 42.5 according to standard STN P ENV 197-1), quartz sand of a continuous granulometry (STN 72 1208) and water. The compositions of mixes are shown in Table 1.

Two samples were made from each mixture, they were left in the mold at room temperature (20°C) under ca. 98% RH conditions for 24 hours. After demolding one specimen series (marked A) was stored in water at 20°C (water storage) and the second sample series (marked B) was cured in an environment with 55% RH and 20°C (air storage) for period up to 28 days.

The standard test of workability (STN 72 2441) was performed on the fresh mortars. Table 1 shows these results, which were intended to only give an indication of the fresh mixes' properties but will not be commented on further.

TABLE 1

Composition and the Workability of Fresh Mortar Mixes

| Mortar | sand/cement ratio | water/cement ratio | consistency (mm) |
|---|---|---|---|
| 2/4 | 2 | 0.4 | 172 |
| 2/5 | 2 | 0.5 | >240 |
| 3/4 | 3 | 0.4 | 106 |
| 3/5 | 3 | 0.5 | 154.5 |
| 3/6 | 3 | 0.6 | 230 |
| 4/5 | 4 | 0.5 | 110 |
| 4/6 | 4 | 0.6 | 138.5 |
| 4/7 | 4 | 0.7 | 187 |
| 6/7 | 6 | 0.7 | 104.5 |

TABLE 2

Physical Properties of Hardened Mortars (A-Water Storage, B-Air Storage) After 28 Days of Curing

| Mortar | Moisture content (mass %) | | Bulk weight $V_d$ ($kg.m^{-3}$) | |
|---|---|---|---|---|
| | A | B | A | B |
| 2/4 | 6.54 | 4.71 | 2119 | 2051 |
| 2/5 | 11.49 | 3.94 | 1977 | 1999 |
| 3/4 | 8.14 | 3.23 | 2010 | 2045 |
| 3/5 | 8.81 | 3.31 | 2026 | 2048 |
| 3/6 | 10.76 | 2.81 | 1969 | 1967 |
| 4/5 | 7.58 | 2.38 | 2055 | 2047 |
| 4/6 | 9.11 | 2.81 | 2055 | 2013 |
| 4/7 | 9.80 | 3.61 | 1964 | 1986 |
| 6/7 | 8.20 | 2.24 | 1964 | 1998 |

On the hardened test samples (after 28 days curing) the volume weight, the content of evaporable water and absorption capacity (by boiling distilled water) were determined before the permeability measurement. The results of these measurements are shown in Table 2.

Permeability Measurement and Calculation of Permeability Coefficient. The water permeability tests were performed using an apparatus similar to that reported elsewhere (15). Sealing of the specimen inserted in a steel ring was achieved with the aid of a silicone sealant. The low pressure gradient of 0.2MPa carried out by compressed air was used to force the water through the specimen. The rubber pads on both sides of the specimen surface prevented the sample from breaking. The specimens were dried at 105°C before the testing.

It is known that a long time is required to achieve equilibrium flow of water through a mortar or concrete specimen and the steady state water flow is usually used for obtaining non-erroneous results. The permeability apparatus used in this investigation measures the quantity of water absorbed with time under conditions which approach non-steady state. Such permeability measurements accelerated the test procedure significantly. The permeability was calculated according to equation on the basis of Darcy's law (3):

$$K = \frac{Q \,.\, I}{A \,.\, P} \tag{1}$$

where K is the permeability coefficient ($m.s^{-1}$), Q is water flow rate ($m^3.s^{-1}$), I is the specimen thickness (m), A is cross-sectional area of the specimen ($m^2$) and P is the pressure head in water column (m). If the pressure used (in MPa) is expressed in unit of the water-column height i.e. 0.2MPa = 20.4m, the following form of equation (1) may be presented:

$$K = \frac{Q \,.\, I}{20.4\,A} = 0.049\,\frac{Q \,.\, I}{A} \tag{2}$$

TABLE 3

Experimental Results of the Permeability Measurement

| Mortar | Absorption capacity N (mass %) | Absorption capacity $N_v$ (volume %) | Time (s) | Permeability coefficient $\times 10^{-10}$ ($m.s^{-1}$) |
|---|---|---|---|---|
| 2/4 A | 6.09 | 12.90 | 22500 | 3.27 |
| 2/4 B | 7.85 | 16.10 | 4500 | 11.67 |
| 2/5 A | 10.40 | 20.56 | 16200 | 4.17 |
| 2/5 B | 11.61 | 23.21 | 4200 | 18.77 |
| 3/4 A | 8.14 | 16.36 | 10800 | 5.71 |
| 3/4 B | 10.18 | 20.82 | 1200 | 48.50 |
| 3/5 A | 8.15 | 16.51 | 13620 | 5.54 |
| 3/5 B | 9.84 | 20.15 | 3300 | 22.81 |
| 3/6 A | 10.17 | 20.02 | 11400 | 7.61 |
| 3/6 B | 12.02 | 23.64 | 2100 | 42.45 |
| 4/5 A | 9.72 | 19.97 | 3000 | 22.18 |
| 4/5 B | 10.86 | 22.23 | 900 | 68.32 |
| 4/6 A | 8.73 | 17.50 | 8280 | 9.13 |
| 4/6 B | 10.57 | 21.28 | 780 | 84.85 |
| 4/7 A | 9.80 | 19.25 | 6300 | 9.73 |
| 4/7 B | 10.72 | 21.29 | 900 | 83.98 |
| 6/7 A | 10.24 | 20.11 | 1980 | 33.89 |
| 6/7 B | 11.02 | 22.02 | 180 | 349.14 |

The Q value is the volume of water, which flows through the specimen thickness at time t (s). These Q values were determined from the difference of both dry (before measurement) and water-saturated (after measurement) weight of specimen divided by time t.

The results of the measurement of mortar specimen permeability are given in Table 3.

It can be seen from these data that the K values vary between 3.27 and 33.89 × $10^{-10}$ $m.s^{-1}$—for water cured specimens, i.e., by one order of magnitude, and between 11.67 and 349.14 × $10^{-10}$ $m.s^{-1}$—for air cured specimens, i.e., one and one-half order of magnitude.

Pore Structure Parameters Determination. In the first approach the absorption capacity value seems to be the simplest measure of open porosity of tested mortars. However, this structure parameter is not sufficiently "correct" since not all open pores are closely related to water permeability. From this point of view good correlation between the values of absorption capacity and permeability coefficient cannot be expected.

The absorption capacity by boiling water which values are shown in Table 3 was determined as follows: the dried specimen was boiled in distilled water for four hours and then cured in the same water during twenty hours. The absorption capacity N was calculated:

$$N = 100.(M_w - M_d)/M_d \quad (\%\text{-mass}) \tag{3}$$

where $M_w$, $M_d$ are the weights of water saturated and dried specimens respectively. Since it is suitable to use the absorption capacity values in volume percentage, the "volume absorption capacity" $N_v$ may be expressed as follows:

$$N_v = N \cdot V_d \quad \text{(\%-volume)} \tag{4}$$

where $V_d$ is the volume weight of the dry specimen. Clearly $N_v$ can be regarded as the apparent porosity of porous material tested and represents the total volume of opened pores. The data of $V_d$ and Nv are shown in Table 2 and Table 3, respectively.

The basic pore structure parameters were estimated from the pressure-volume data of the series 2000 mercury intrusion porosimeter and micropore unit 120 f.ERBA Science, enabling the determination of micropores with the radius from 3.7 nm up to 7500 nm and of larger pores with a radius up to 0.6 mm. The porosimetry measurements were carried out by the fraction of broken dried samples after the determination of water content in water saturated samples after the finishing of the permeability measurement. The following pore structure parameters were estimated by (MIP) used:

$V_{TP}$-total pore volume ($mm^3.g^{-1}$)
$V_{MP}$-volume of micropores; range of 3.7-7500nm ($mm^3.g^{-1}$)
TP-total porosity (% vol.)
$M_{TP}$-total pore radius median (nm)
$M_{MP}$-micropore radius median (nm)
S-pore surface area-cylindrical model ($m^2.g^{-1}$)
$F_x$-frequency of occurrence of pores in different size ranges

The results of the pore structure characteristics measurements are shown in Table 4.

## Results and Discussion

Process of the Effective Pore Structure Parameter Searching. Many structural parameters of cementitious materials are available from MIP or other laboratory techniques results. However one individual pore structure parameter cannot fully describe the pore structure sufficiently. It is generally agreed that pore size represents the most suitable single pore structure parameter for expressing of relation between pore structure and permeability. It seems to be a better parameter than pore quantity.

In order to confirm these assertions, linear regression analysis was used for evaluation of the closeness of relation between pore structure parameters such as apparent ($N_V$) and total porosity (TP), volume of micropores ($V_{MP}$), pore surface area (S), total pore radius median ($M_{TP}$) and micropore radius median ($M_{MP}$) and permeability coefficient.

The results of the regression analysis of the functional relation

$$\log K = \log(PS) \tag{5}$$

where K is the permeability coefficient and PS is pore structure parameter ($N_V$, TP, $V_{MP}$, S, $M_{TP}$, $M_{MP}$) are shown in Table 5.

Two important facts are evident from these results: first— only parameter S (pore surface area) from the groups I and II, which is related to quantity of pores indicates a relatively good correlation to permeability and second—the micropore radius median $M_{MP}$ seems to be the parameter with the closest relation to permeability. The following conclusion can be drawn from the results: It means that the range of micropores (3.7-7500 nm) is the first approaching the "relevant" pore range.

TABLE 4

The Results of the Structural Measurements of Mortars

| Mortar | Pore volume | | Micro-pore radius median | Pore radius median | Total porosity | Pore surface area | Pore structure parameter |
|---|---|---|---|---|---|---|---|
| | micro-pores $V_{MP}$ ($mm^3.g^{-1}$) | all pores $V_{TP}$ ($mm^3.g^{-1}$) | $M_{MP}$ (nm) | $M_{TP}$ (nm) | TP (vol. %) | S ($m^2.g^{-1}$) | $VM_F$ (nm) |
| 2/4 A | 59.9 | 63.3 | 60.7 | 63.5 | 13.63 | 2.824 | 12.74 |
| 2/4 B | 59.7 | 62.3 | 70.6 | 75.1 | 13.60 | 2.693 | 22.86 |
| 2/5 A | 70.9 | 77.9 | 65.4 | 72.8 | 14.68 | 3.248 | 13.17 |
| 2/5 B | 67.9 | 78.7 | 128.9 | 180.0 | 15.50 | 3.200 | 37.88 |
| 3/4 A | 43.9 | 54.4 | 71.7 | 147.4 | 12.10 | 3.267 | 15.40 |
| 3/4 B | 34.7 | 39.2 | 253.8 | 399.9 | 8.85 | 1.350 | 54.40 |
| 3/5 A | 48.7 | 51.2 | 68.1 | 71.5 | 11.37 | 3.541 | 16.50 |
| 3/5 B | 50.1 | 54.5 | 152.8 | 178.6 | 12.02 | 3.106 | 47.75 |
| 3/6 A | 70.1 | 72.3 | 65.0 | 67.4 | 15.33 | 3.033 | 15.92 |
| 3/6 B | 75.0 | 78.4 | 220.7 | 262.1 | 16.49 | 3.289 | 94.24 |
| 4/5 A | 51.9 | 56.2 | 140.7 | 181.0 | 12.38 | 3.230 | 42.88 |
| 4/5 B | 38.2 | 49.6 | 492.3 | 1221 | 11.16 | 1.616 | 118.01 |
| 4/6 A | 75.9 | 78.8 | 74.4 | 79.3 | 16.54 | 3.447 | 27.76 |
| 4/6 B | 61.0 | 67.2 | 217.4 | 301.6 | 14.43 | 1.912 | 81.64 |
| 4/7 A | 66.3 | 68.8 | 78.1 | 82.6 | 14.64 | 2.765 | 22.90 |
| 4/7 B | 64.1 | 67.3 | 220.2 | 250.6 | 14.41 | 1.771 | 93.69 |
| 6/7 A | 60.1 | 68.6 | 126.1 | 201.4 | 14.70 | 2.407 | 41.99 |
| 6/7 B | 50.8 | 60.1 | 709.1 | 1128 | 13.13 | 1.656 | 243.05 |

TABLE 5

The Structural Parameters Measured and the Results of Regression Analysis

| Group of structural parameters | The group is related to: to: | Pore structure parameter | Correlation coefficient |
|---|---|---|---|
| I. Pore volume | quantity of pores | $N_V$ - absorption capacity | 0.468 |
| | | TP - total porosity | 0.019 |
| | | $V_{MP}$ - volume of micropores | 0.055 |
| II. Surface area | quantity of pores | S - pore surface area | 0.643 |
| III. Pore size | pore size distribution | $M_{TP}$ - pore radius median | 0.794 |
| | | $M_{MP}$ - micropore radius median | 0.891 |

It can be assumed that the suitable and representative pore structure parameter searched must inevitably contain the following individual structural parameters which sufficiently objectively and effectively characterize the whole pore system from the permeability processes point of view:

1. The total volume of open pores, i.e., "open" porosity—$V_{OP}$
2. The volume of pores that are the most responsible to permeability i.e. "relevant" porosity—$V_{RP}$/the portion of the volume of micropores $V_{MP}$ in the total porosity TP, as is expressed by equation (7)
3. Micropore radius median—$M_{MP}$

On the basis of analysis of knowledge about pore structure parameters, a product of pore volume and pore median for a suitable pore structure parameters has been assumed. It was estimated empirically, however, that a more suitable one is a product of micropore median value and the ratio of the volumes of relevant pores ($V_{RP}$) and total ones ($V_{OP}$):

$$VM = \frac{V_{RP}}{V_{OP}} \times M_{MP} \quad \text{(nm)} \tag{6}$$

where $V_{RP}$ expresses the equation:

$$V_{RP} = \frac{V_{MP}}{V_{TP}} \times TP \quad (\%) \tag{7}$$

and $V_{OP}$ to the apparent porosity $N_V$ is equal.

Fitness of VM for the expression of relationship between permeability coefficient K and the quality of the given pore structure shows the equation:

$$\log K = f\{\log (V_{RP} / V_{OP}) \times M_{MP}\} \tag{8}$$

with correlation coefficient of 0.883. This value is relatively good, confirming the mentioned fitness.

The Improvement of the Correlation between VM and K by Involving of the "Effective" Pore Size Range. The mentioned improvement represented the following procedure: (1) the choice of six different pore radius ranges (>100nm, 100-6000nm, 60-10000nm, 100-10000nm, 180-10000nm and 100-18000nm); (2) an expression of pore size distribution data ascertained from MIP, by means of frequencies of occurrence of the pores of the mentioned size ranges. These frequencies as dimensionless values in the scale from 0 to 100 are given in Table 6.

The frequency of occurrence of micropore volume in different pore size ranges is given by the equation:

$$V_{EF} = \frac{V_{RP}}{V_{OP}} \times \frac{Fx}{100} \tag{9}$$

TABLE 6

Frequency of Occurrence of Pores in Different Size Ranges

| Mortar | >100nm | | 100 - 6000nm | | 60 - 10000nm | | 100 - 10000nm | | 180 - 10000nm | | 100 - 18000nm | |
|---|---|---|---|---|---|---|---|---|---|---|---|---|
| | A | B | A | B | A | B | A | B | A | B | A | B |
| 2/4 | 27 | 44 | 21 | 39 | 53 | 58 | 21 | 40 | 14 | 28 | 23 | 41 |
| 2/5 | 37 | 62 | 29 | 49 | 55 | 61 | 31 | 51 | 14 | 39 | 34 | 55 |
| 3/4 | 53 | 67 | 34 | 54 | 46 | 63 | 36 | 57 | 29 | 50 | 39 | 61 |
| 3/5 | 40 | 62 | 36 | 56 | 56 | 67 | 37 | 57 | 26 | 44 | 38 | 59 |
| 3/6 | 36 | 68 | 33 | 63 | 56 | 74 | 33 | 64 | 17 | 53 | 34 | 65 |
| 4/5 | 60 | 80 | 51 | 56 | 63 | 68 | 53 | 62 | 44 | 55 | 56 | 70 |
| 4/6 | 44 | 67 | 41 | 58 | 58 | 72 | 41 | 61 | 28 | 50 | 42 | 63 |
| 4/7 | 44 | 69 | 40 | 65 | 59 | 74 | 40 | 66 | 23 | 54 | 41 | 67 |
| 6/7 | 62 | 79 | 49 | 62 | 64 | 75 | 52 | 68 | 42 | 61 | 55 | 74 |

The relationship between VM, micropore median $M_{MP}$ and permeability coefficient K is given by the equation:

$$\log K = f(\log VM_F) = f\{\log (V_{EF} \times M_{MP})\} \quad (10)$$

The values of the correlation coefficient of this relation are shown in Table 7.

It is evident that the range of pore radius between 100 and 10000nm reaching the highest values of the correlation coefficient, represents the most significant pore radius range having the deciding influence on the permeability of the given pore structure. Taking it into account Equation 6 can be expressed as:

$$VM_F = \frac{V_{RP}}{V_{OP}} \times (F_{100-10000}) \times M_{MP} \times 10^{-2} \quad \text{(nm)} \quad (11)$$

where $F_{100-10000}$ is the frequency of occurrence of pores in the radius range of 100-10000 nm.

TABLE 7

Correlation Coefficient of the Functional Relationship logK = log($VM_F$) for Various Ranges of Pore Radius

| Pore radius range (nm) | Correlation coefficient |
|---|---|
| 3.7 - 7500 | 0.883 |
| 60 - 10000 | 0.902 |
| > 100 | 0.938 |
| 100 - 6000 | 0.949 |
| 100 - 10000 | 0.953 |
| 180 - 10000 | 0.936 |
| 100 - 18000 | 0.901 |

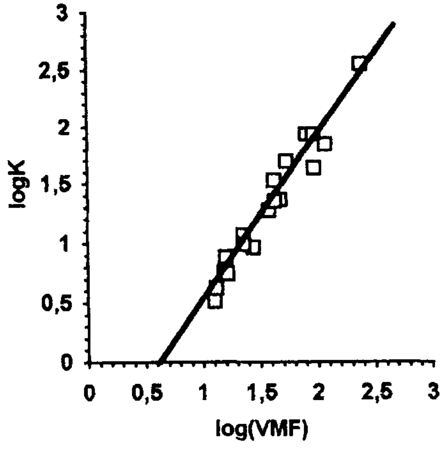


FIG. 1.
Relationship between permeability and new pore structure parameter.

For the regression equation:

$$\log K = 1.438 \log (VM_F) - 0.971 \qquad (12)$$

a correlation coefficient of 0.953 has been obtained. This is a significantly better value than in the case of Eq. 6, which does not consider the frequency factor. Therefore Eq. 11 for the improvement of the relationship (6) can be considered.

The linear relationship between the logK and log ($VM_F$) is shown in Figure 1.

It is clear from Eq. 11 that all members representing the new pore structure parameter $VM_F$—with the exception of a $V_{OP}$ (absorption capacity $N_V$)—by mercury intrusion porosimetry were estimated. In practice, however, for more simple and quick evaluation of permeability the only application of MIP data seems to be more advantageous.

Therefore a modified pore structure parameter $VM^*_F$ was defined to estimate the closeness of the correlation logK = f(log$VM^*_F$). With this modification, Eq. 11 becomes:

$$VM^*_F = V_{RP} \times (F_{100\text{-}10000}) \times M_{MP} \times 10^{-2} \qquad (13)$$

With this alteration, the water permeability has been calculated according to equation:

$$\log K = 1.2634 \log (VM^*_F) - 2.323 \qquad (14)$$

with the correlation coefficient of 0.943.

So, significant linear correlations were observed between the permeability of cement mortars and pore structure as determined by MIP. These results suggest that the empirical equations (12,14) may be used to a simple, quick and realistic evaluation of permeability of cementitious materials.

## Conclusions

1. An empirical expression has been derived using mercury intrusion porosimetry data to describe the pore system in cement-based materials. From this expression the water permeability coefficient according to a simple functional equation can be easily calculated.
2. Micropores up to 7500nm in radius are the "relevant" range in relation to permeability. Better limits for this pore range of 100-10000nm are suggested.
3. The product of the portion of micropore volume in the total open pore volume and micropore radius median derived in this paper seems to be the suitable parameter for the expression of the relationship between permeability and pore structure.
4. The advantage of this presented procedure is that all pore structure parameters in the expression of $VM^{*}_{F}$ used are precisely defined and only by mercury intrusion porosimetry estimated.
5. The authors supposed that the generalized form of the expression $V_{RP}xF_{x}xM_{MP}$ should be used to the evaluation or prediction of other physical properties of cement-based materials, which are closely related to the pore structure (strength, durability).
6. To make the results obtained more exact it would be desirable to perform permeability and pore structure measurements by at least three tests for each specimen and to determine the permeability coefficient by steady-flow state procedure.

## Acknowledgments

The authors are grateful to grant agency VEGA (grant no. 2/4087/97) for partial supporting of this work.

## References

1. B.K. Nyame, J.M.Illston, Relationships between permeability and pore structure of hardened cement paste, Mag.Concr.Res., 33, 116, 139-146, (1981).
2. S. Li, D.M. Roy, Investigation of relations between porosity, pore structure, and $Cl^-$ diffusion of fly ash and blended cement pastes, Cem.Concr.Res., 16, 5, 749-759, (1986).
3. B.K. Nyame, J.M. Illston, Capillary pore structure and permeability of hardened cement paste, 7th International Symposium of the Chemistry of Cement, Paris, III, VI 181-186, 1980.
4. P.K. Mehta, D. Manmohan, Pore distribution and permeability of hardened cement pastes, 7th International Symposium of the Chemistry of Cement, Paris, III, VII 1-5, 1980.
5. S. Goto, D.M. Roy, The effect of w/c ratio and curing temperature on the permeability of hardened cement paste, Cem.Concr.Res., 11, 4, 575-579, (1981).
6. R.S. Mikhail, D.H. Turk and S. Brunauer, Dimensions of the average pore, the number of pores, and the surface area of hardened portland cement paste, Cem.Concr.Res., 5, 5, 433-442, (1975).
7. D.C. Hughes, Pore structure and permeability of hardened cement paste, Mag.Concr.Res., 37, 133, 227-233, (1985).
8. D.M. Roy, Relationships between permeability, porosity, diffusion and microstructure of cement pastes, mortar, and concrete at different temperatures, R.L. Roberts and J.P. Skalny, Ed., Mater.Res. Soc. Symp. Proc., 137, Boston, 179-189, 1988.
9. B. Meng, Resolution-dependent characterization of interconnected pore systems: development and suitability of a new method, Mat. and Str., 27, 63-70, (1994).

10. R.F. Feldman, Pore structure, permeability and diffusivity as related to durability, 8th Int. Congr. Chem. Cem., I, Rio de Janeiro, 337-356, 1986.
11. E.J. Garboczi, Permeability, diffusivity and microstructural parameters: a critical review, Cem.Concr.Res., 20, 4, 591-601, (1990).
12. T. Luping, L.O. Nilsson, A study of the quantitative relationship between permeability and pore size distribution of hardened cement pastes, Cem.Concr.Res., 22, (4) 541-559, (1992).
13. A.S. El Dieb, R.D. Hooton, Evaluation of the Katz-Thompson model for estimating the water permeability of cement based materials from mercury intrusion porosimetry data, Cem.Concr.Res., 24, (3) 443-455, (1994).
14. P.W. Brown, D. Shi, J. Skalny, Porosity/permeability relationships, Mat.Sci.Concr. II, J. Skalny and S. Mindess, Ed., ACS, 83-110, 1991.
15. H. Gräf, H. Grube, Verfahren zur Prûfung der Durchlässigkeit von Mörtel und Beton gegenûber Gasen und Wasser, Beton, 36, (5) 184-187, (1986).